

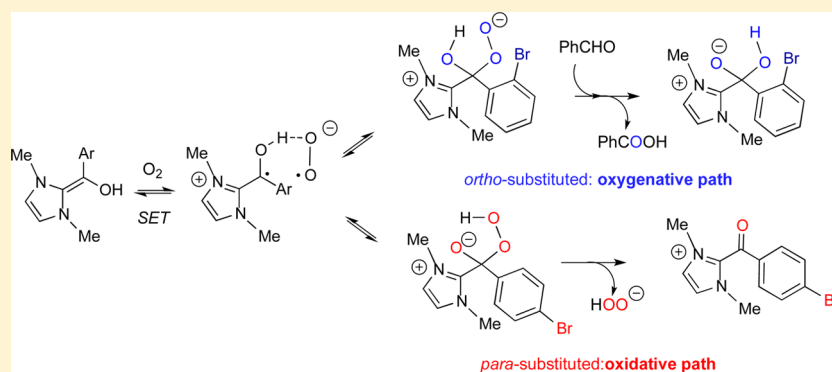
Formation, Oxidation, and Fate of the Breslow Intermediate in the *N*-Heterocyclic Carbene-Catalyzed Aerobic Oxidation of Aldehydes

Olga Bortolini,^{*,†} Cinzia Chiappe,[‡] Marco Fogagnolo,[†] Alessandro Massi,[†] and Christian Silvio Pomelli^{*,‡}

[†]Dipartimento di Scienze Chimiche e Farmaceutiche, Università di Ferrara, Via Fossato di Mortara 17-19, 44121 Ferrara, Italy

[‡]Dipartimento di Farmacia, Università di Pisa, Via Bonanno 33, 56126 Pisa, Italy

S Supporting Information



ABSTRACT: The reaction paths and intermediate structures related to the formation of the Breslow intermediate and its oxidation along the oxidative/oxygenative lanes have been studied from a mechanistic point of view, with the support of gas-phase and computational studies. The results confirm the occurrence of a single-electron transfer from the Breslow intermediate to the molecular oxygen with formation of a radical couple that recombines either as a peroxide anion 7' to afford the aldehyde-to-carboxylic acid product or as a hydroperoxy derivative 7'' that evolved into an electrophilic acyl azolium, opening to the aldehyde-to-ester conversion. Steric factors enter into determining the different reactivity. All of the intermediates of both catalytic paths have been observed and characterized under mass spectrometric conditions. In particular, for the imidazoline catalyst, the (+)ESI-MS/(MS) detection of the genuine Breslow intermediate was made possible in virtue of its limited reactivity. Mechanistic aspects of the *N*-heterocyclic carbenes catalyzed aerobic oxidation of aldehydes shares important similarities with that one of the recently revisited benzoin condensation.

INTRODUCTION

N-Heterocyclic carbenes (NHCs) are a particular class of organic compounds widely employed as ligands for their aptitude to coordinate transition metals and as catalysts for their ability to bind to carbon electrophiles.¹ As organocatalysts, NHCs display the remarkable ability to promote the polarity reversal of specific functional groups, in particular aldehydes. This umpolung effect has been explored in many organic transformations, most of them involving the initial nucleophilic attack of the carbene **1** to the carbonyl group of **2** (Scheme 1). As proposed by Breslow,² along the lines of the Lapworth's cyanide mechanism,³ an intramolecular,⁴ intermolecular,⁵ or solvent-mediated proton transfer⁶ in the adduct **3** generates the amino enol **4**, known as the Breslow intermediate, which is nucleophilic at the C(1) carbon.^{7,8} Subsequent nucleophilic attack to a second aldehyde molecule with formation of a new C–C bond and release of the NHC catalyst affords the benzoin product **6**.

Although postulated in 1958, the first successful generation of the amino enol **4** from aldehydes and carbenes and its

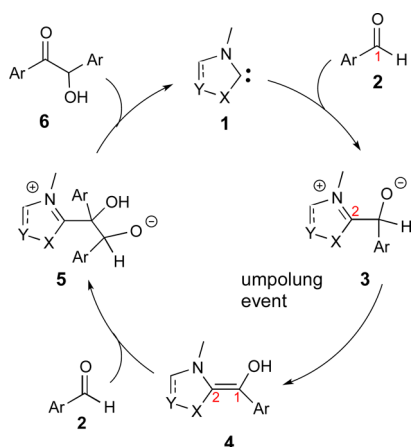
characterization by in situ NMR spectroscopy was reported only in 2012.⁹ Studies on the observation and evaluation of the nucleophilicity of related deoxy and methoxy Breslow-like compounds,^{10,11} as well as the characterization of sila-Breslow intermediates, have been also carried out.¹²

This prominent chemistry, of which the benzoin condensation and Stetter reaction are the archetypal examples, has been recently enriched with oxidative protocols for the direct construction of different classes of compounds, principally acids, esters, and amides.¹³ All of these oxidative NHC-mediated reactions share a common key event, represented by the oxidation of the Breslow intermediate **4**, that occurs in the presence of inorganic or organic oxidants, including O₂. In the majority of cases, **4** is converted into the corresponding electrophilic acylazolium ion **10**, which may be easily intercepted by nucleophiles; however, not all of the oxidations necessarily proceed in this direction.¹⁴ When oxygen is used as

Received: October 4, 2016

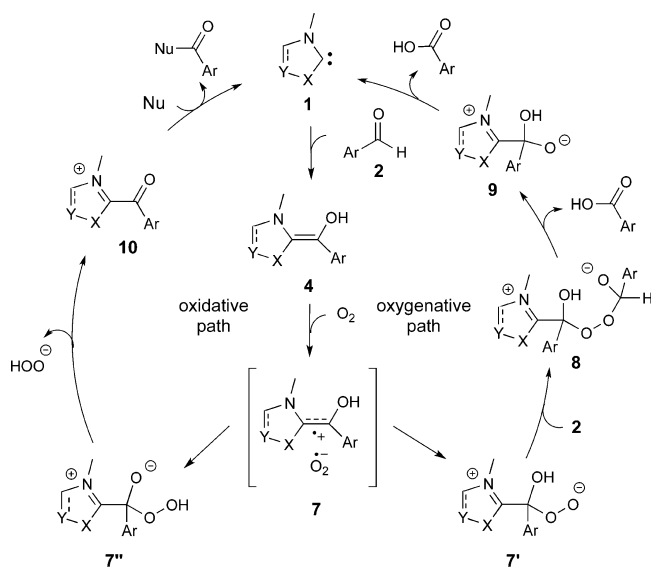
Published: December 14, 2016

Scheme 1. Commonly Proposed Mechanism for the Benzoin Condensation



oxidant, activation of O_2 can occur with formation of the complex **7** that after radical recombination may evolve to the peroxide anion $7'$ or to the hydroperoxy intermediate $7''$ (Scheme 2). In a recent mass spectrometric investigation on

Scheme 2. Proposed Mechanisms for the NHC-Catalyzed Aerobic Oxidation of Aldehydes (Oxygenative and Oxidative Paths)



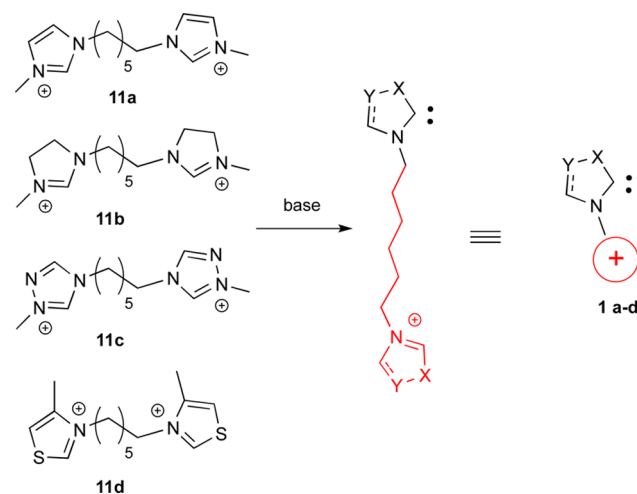
the NHC-catalyzed oxidative transformation of aldehyde substrates, the isobaric intermediates $7'$ and $7''$ have been intercepted and their reactivity characterized.^{14a} Depending on steric factors, the complex **7** is prone to evolve into the intermediate **8** by reaction of $7'$ with an additional aldehyde molecule in a process reminiscent of the Baeyer–Villiger oxidation. The rearrangement of **8** gives rise to a carboxylic acid and the oxo-Breslow **9** that completed the cycle by reforming the NHC catalyst **1** through release of a second molecule of acid (oxygenative path). Alternatively, **7** converts into the acyclic cation equivalent **10**, through the intermediate $7''$, with liberation of the hydroperoxy anion (oxidative path).

Despite efforts to observe the genuine Breslow intermediate **4** in the gas phase, however, all attempts met with failure.^{12,14a,15,16}

In the present study, we approached the problem by playing on the different reactivity of the NHC catalysts both in solution and the gas phase, in parallel with computational studies. In particular, we investigated the detailed mechanism of formation of the Breslow intermediate and its oxidation along the oxygenative/oxidative paths, explaining the key factors that control the formation of the peroxidic species $7'$ and $7''$ via a single-electron-transfer (SET) process with O_2 and their evolution toward the observed divergent reactivity under aerobic conditions. Gas-phase studies and theoretical calculations unequivocally support the involvement of an oxidative SET¹⁷ during the activation of molecular oxygen, and the proposed mechanism shares important similarities with that one of the recently revisited benzoin condensation.^{8a}

RESULTS AND DISCUSSION

The possibility of studying a reaction in the gas phase is intimately linked to the presence of charged species. Since all of the intermediates involved in the catalytic cycles depicted in Scheme 2 are neutral, suitable carbene precursors bearing a charged moiety for mass spectrometric detection are required. Bis-diazolium derivatives are particularly appropriate for the role, and therefore, we synthesized the *N*-methylated 1,1'-(hexane-1,6-diyl)azolium salts of the most common heterocyclic scaffolds imidazole **11a**, imidazolium **11b**, triazole **11c**, and the thiazole compound **11d**, in combination with different counterions, i.e., Tf_2N^- , PF_6^- , and glutarate (Scheme 3). The dual role of these bis-azolium derivatives is that of precursors of the carbene catalysts **1a–d** and, in the meantime, of charge-tags.^{12,14a,18}

Scheme 3. Structure of the NHC Catalysts Used in the Study^a

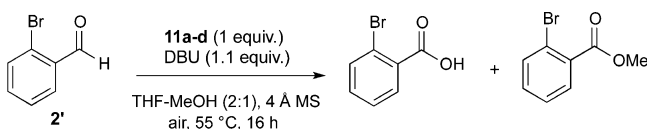
^aTheazolium salts have been numbered on the basis of the heterocycle typology, independently from the anionic counterpart.

Oxidative Conversion of *o*-Bromo **2'** and *p*-Bromo-benzaldehydes **2''** and ESI MS Investigation.

As anticipated, during the oxidative conversion of aromatic aldehydes using **11a** as precatalyst in THF–MeOH (2:1) and DBU as base, we observed a significantly different product distribution switching between *ortho*-substituted and *para*-substituted benzaldehydes. As an example, the ratio between methyl ester/carboxylic acid changes from 5:47 to 89:11 on going from *o*-bromo- **2'** to *p*-bromobenzaldehyde **2''**. Hence,

our investigation commenced with the evaluation of the activity of the different azolium catalysts **1a–d** in solution using **2'** and **2''** as exemplary substrates. Table 1 collects the results that pertain to the oxidation of the *ortho* derivative.

Table 1. Oxidation–Esterification of Aldehyde **2'^a**



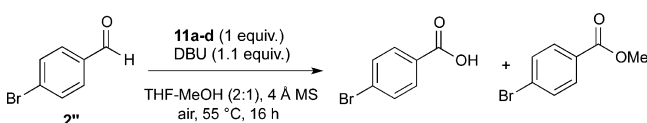
entry	NHC ^b	unreacted 2' ^c (%)	acid ^c (%)	ester ^c (%)
1	1a (X = PF ₆)	18	41	5
2	1a (X = glutarate)	12	47	5
3	1b (X = PF ₆)	91	5	
4	1c (X = PF ₆)	23	19	21
5	1c (X = Tf ₂ N)	16	17	25
6	1d (X = PF ₆)	24	21	8

^aSee the Experimental Section for details. ^bObtained from the corresponding precursors **11a–d** associated with different anions X. ^cIsolated yield.

Collectively, the oxidative reaction of **2'** is low yielding, and the conversion of the substrate never reaches completeness, also after 16 h reaction time. Notable, however, is the acid-over-ester formation found for **1a**, **1b**, and **1d**, whereas **1c** was less selective, affording almost equal amounts of acid and ester (entries 4 and 5). These findings are consistent with literature data reporting discrete amounts of ester formation during the oxidative conversion of *ortho*-substituted aromatic aldehydes in the presence of triazolium precatalysts.¹⁴ The catalysts activity sequence is in the order imidazole, triazole, thiazole, and imidazoline derivative **1b**, as the poorest reactive catalyst (entry 3).

p-Bromobenzaldehyde **2''** was found to be more reactive than the *ortho*-substituted counterpart, affording good to excellent yields of the methyl ester, as shown in Table 2. The

Table 2. Oxidation–Esterification of Aldehyde **2''^a**



entry	NHC ^b	unreacted 2'' ^c (%)	acid ^c (%)	ester ^c (%)
1	1a (X = PF ₆)	22	18	60
2	1a (X = glutarate)		11	89
3	1a (X = Tf ₂ N)	11	14	75
4	1b (X = PF ₆)	88	2	10
5	1c (X = PF ₆)		11	89
6	1c (X = Tf ₂ N)		7	93
7	1d (X = PF ₆)		23	77

^aSee the Experimental Section for details. ^bObtained from the corresponding precursors **11a–d** associated with different anions X. ^cIsolated yield.

limited catalytic activity of **1b** is also confirmed in this case, opening to the direct observation and characterization of the Breslow intermediate **4b**, as discussed later on. Furthermore, the results indicate a minor effect of the azolium salt anion X^{n−}, either singly or doubly charged, on the reaction.

The results shown in Tables 1 and 2 document the divergent oxidative reactivity of substituted aromatic aldehydes for the most commonly used NHC catalysts as dependent on the position of the substituent on the aromatic ring.¹⁹

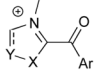
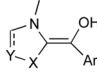
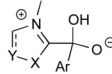
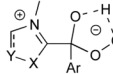
In the mechanistic proposal depicted in Scheme 2, the pivoting intermediates in this oxidative transformation are the peroxidic Breslow derivatives **7'** and **7''**, formed from the Breslow intermediate **4** by addition of molecular oxygen. This activation is believed to proceed via a single-electron-transfer (SET) processes with O₂ to give the complex **7** formed by the radical cation [4]^{•+} and the superoxide radical anion [O₂]^{•−} that recombine to afford **7'** or **7''**.²⁰ We have calculated the structure of the complex between [4]^{•+} and [O₂]^{•−} and found that a fraction of the oxygen spin density spreads on [4]^{•+}, mainly on the C(2) atom (see the computational discussion for details). The peroxo Breslow intermediates are characterized by a divergent reactivity either as a peroxide anion **7'** affording the aldehyde-to-carboxylic acid product or as hydroperoxy derivative **7''** with the formation of the ester product. This dual reactivity is earmarked by specific intermediates that should be observed in the gas phase: the elusive Breslow **4**, the isobaric peroxidic derivatives **7'/7''**, common species of the overall mechanism, and either the oxo Breslow **9** or the acyl intermediate **10** that should be preferably intercepted when the oxygenative or oxidative paths of Scheme 2 are occurring. Table 3 collects the relative amounts of the mentioned intermediates, as observed by (+)-ESI-MS experiments carried out using aldehydes **2'** (entries 1–4) and **2''** (entries 5–8).

The mass spectrometric results are fully consistent with the reactivity found in solution. With the *ortho*-substituted benzaldehyde **2'**, all the catalyst typologies afford consistent amounts of the oxo Breslow **9a–d** suggestive of the preferred acid formation. On the other hand, this same intermediate is barely detectable with *p*-bromobenzaldehyde **2''** in favor of the formation of the acyl species **10a–d**. The triazole-based catalyst **1c** is the only example for which the acyl intermediate **10c** and **9c** coexist, indicating the concurrent presence of both reactivities, as actually found.

A remarkable result of this study is the detection of the genuine Breslow intermediate **4b** made possible by the limited reactivity of **1b**, as shown in Figure 1. It is well established, in fact, that the saturation of C(4)–C(5) bond precludes aromatization, giving the Breslow intermediate a higher stability.^{9a,11b}

To our knowledge, there are only two previous attempts to intercept and characterize the Breslow intermediate using mass spectrometric techniques. Glorius and co-workers¹⁶ reported the formation of a protonated Breslow-like complex formed from an imidazolium derivative and an α,β -unsaturated aldehyde as model for the “conjugate” umpolung. The group of Lee¹⁵ described the formation of an adduct between a thiazolium carbene containing a sulfonate charge tag and benzaldehyde. In this latter case, the easy release of the benzaldehyde with reformation of the NHC catalyst observed in the MS/MS spectrum is more consistent with an addition product prior to the proton transfer, similar to **3** of Scheme 1.¹² In the MS/MS spectrum of **4b** (*m/z* 435 ⁷⁹Br), in contrast, the dissociation back to catalyst **1b** (*m/z* 251) and aldehyde **2'** represents a marginal fragmentation path, attesting a solid connection, likely a double bond, between the carbene and the aldehyde. The cleavage of the imidazolium ring is the relevant event of this MS/MS spectrum, affording the ions at *m/z* 253 and 240, respectively, Figure 2 and Scheme 4.

Table 3. Occurrence of the Most Important Intermediates Detected in (+)-ESI-MS Spectra of Solutions Containing *o*-Bromo-2' or *p*-Bromobenzaldehyde 2'' and the Selected Catalyst 1 Using DBU as Base^{a-d}

Entry	NHC	Aldehyde				
			10a-d	4a-d	9a-d	7'/7''a-d
1	1a	2'	⊗	⊗	+++	+
2	1b	2'	⊗	+	++	+
3	1c	2'	+	⊗	+	⊗
4	1d	2'	⊗	⊗	++	+/-
5	1a	2''	+	⊗	+/-	+/-
6	1b	2''	+/-	⊗	+/-	⊗
7	1c	2''	++ ^d	⊗	+/-	⊗
8	1d	2''	+	⊗	+	⊗

^aSee the [Experimental Section](#) for details. ^bThe charge-tag portion has been omitted for clarity. ^c⊗, not detected. Relative abundance of the MS signal: below 2% (\pm), up to 10% (+); up to 50% (++); up to 100% (+++). ^dFor more MS and MS/MS details and spectra carried out in the absence of MeOH, see the [SI](#).

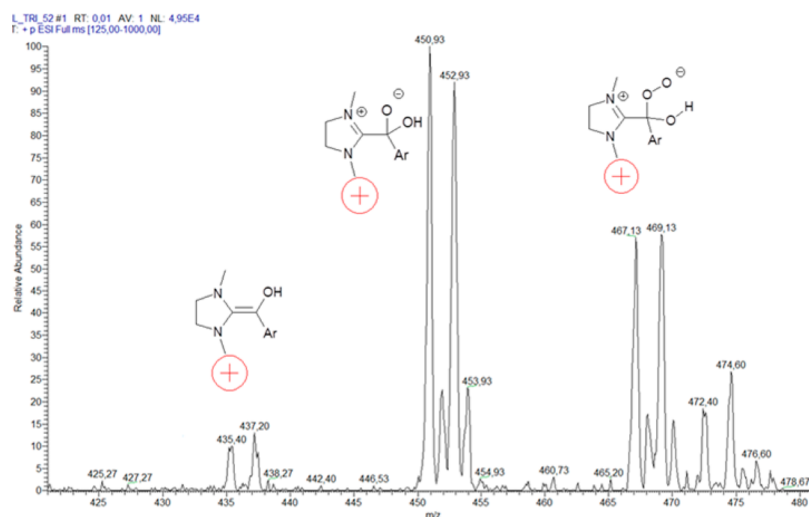


Figure 1. Expanded section of the (+)-ESI-MS full scan of solutions containing *o*-bromobenzaldehyde 2', 11b as precursor catalyst, and DBU, dissolved in THF–MeOH (2:1).

Recent studies have proved the occurrence of the keto tautomer of the Breslow intermediate **12b** under specific conditions as the azole ring typology and a suitable substitution of the heterocyclic nitrogen(s).^{9b,21} According to its structure, ion **12b** would presumably dissociate in the MS/MS experiment by release of the acyl cation ($\text{Br}-\text{C}_6\text{H}_4-\text{CO}^+$) at m/z 183, which however, was observed in very low relative abundance. In contrast, our results are fully consistent with the classical enol structure of the Breslow intermediate.

Formation and Fate of the Breslow Intermediate: Computational Approach. To obtain reliable information from a computational study of chemical reactivity in solution, it is fundamental to define adequately the model system. Since the charged moiety of the tagged NHC **1a–d** is located far from the reactive site, in order to reduce the computational cost, the charged catalyst **1a–d** has been replaced with the simpler *N,N*-dimethylazolium structure (black portion in [Scheme 3](#)). Furthermore, in the framework of the supermolecular approach, widely used in the ionic liquids field,²² we

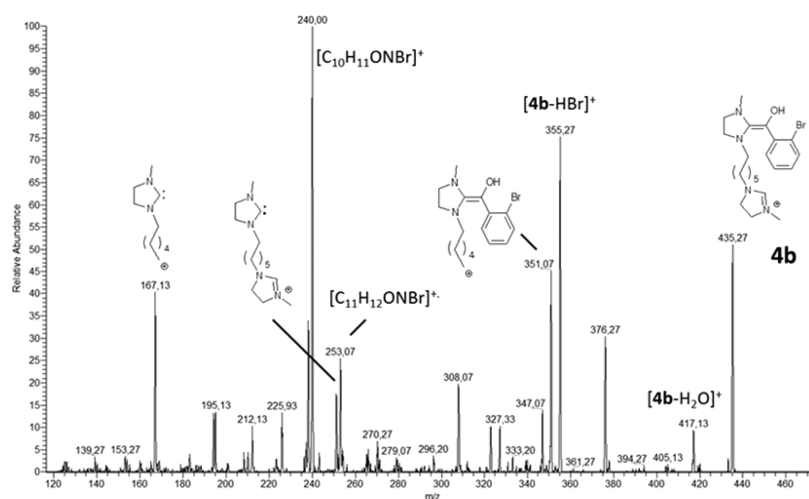
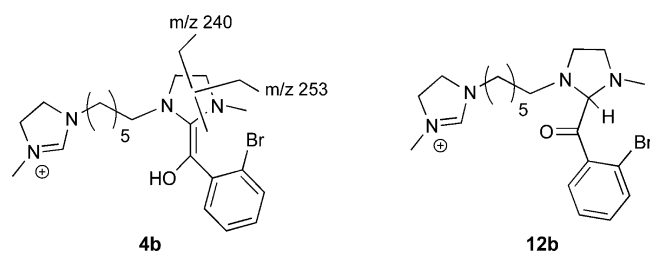


Figure 2. (+)ESI-MS/MS spectrum of the ionic species at m/z 435 (^{79}Br).

Scheme 4. Major Fragmentation Patterns Observed in the MS/MS Spectrum of 4b and Structure of the Keto Form of the Breslow Intermediate 12b



have included five explicit methanol molecules in our model system considering the role that a protic solvent can play in a reaction involving proton transfer and charge reorganization. The five molecules were collocated as follows: one localized in the central part of the reaction site, i.e., hydrogen bonded to the C2 carbon of the carbene catalyst; two methanol molecules were hydrogen bonded to the aldehyde carbonyl oxygen (O1); and two positioned near the bromine substituent on the phenyl ring. All calculations have been performed using the Terachem 1.50 package²³ and the B3LYP/6-311++G(d,p) level of theory. Dispersion corrections according to the D3 Grimme scheme²⁴ have been included. All optimized geometries are reported in the Supporting Information.

The first step of the reaction is the addition of the heterocyclic carbene to the carbonyl group of the *o*-bromobenzaldehyde 2'. An encounter complex (EC(1a-d + 2')) for each heteroazolium has been designed by arranging the two reagent rings (azol-2-ylidene and phenyl) facing each other and the reacting centers (carbonyl and carbene) as close as possible. After structures optimization, the distances between the carbene carbon (C2) and the aldehyde carbonyl carbon (C1) became 3.54 Å. These optimized structures have been taken as the zero energy point (reference). The intermediate 3' (where the apostrophe refers to the complex obtained starting from *ortho*-substituted benzaldehyde 2') with a new single covalent bond between C1 and C2 was obtained starting from the optimized encounter complexes reducing, step by step, the C1–C2 distance and reoptimizing the structure each time. This procedure allowed us to obtain the starting and ending point of the first reaction step. These two points have been used to calculate the reaction path by applying the nudged elastic band

procedure (NEB).²⁵ This reaction path is characterized by the formation of the new C–C bond and by the contemporaneous shift of the methanol molecule, hydrogen bonded to C2 carbene atom, toward one of the methanol molecules coordinated to the aldehyde carbonyl oxygen, O1. To complete the formation of the Breslow intermediate 4' the hydrogen atom, still bonded to C1 in 3', must be transferred to the negatively charged oxygen. This transfer is not direct but mediated by two methanol molecules, as shown in Figure 3.

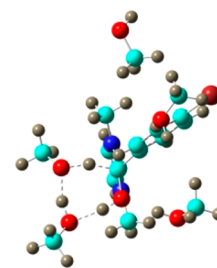


Figure 3. Geometrical arrangement of the methanol-mediated proton transfer that transforms the intermediate 3' into the Breslow intermediate 4'. The apostrophe refers to the complex obtained starting from 2'. The O–H bonds involved in this rearrangement are represented as dotted lines.

The hydrogen atom at C1 migrates to the nearby methanol molecule which, in turn, transfers its hydrogen atom to a second methanol molecule that, finally, donates a proton to quench the negatively charged alkoxide. The whole process is synchronous. The NBO analysis, reported in Table 4, confirms that the transformation of the aldehyde group into the corresponding enol is characterized by the transfer of some charge to the azol-2-ylidene ring, inverting the polarity of the C1 carbon. Only a limited amount of charge migrates to the substituted phenyl ring. On the other hand, transfer of the alcoholic protons occurs without alteration in their polarity.

The relevant energetic parameters of the entire process are summarized in Table 4 and Figure 4. Additional information and absolute energies may be found in the Supporting Information. The addition of carbene 1a–d to *o*-bromobenzaldehyde 2' TS (1+2'→3') is particularly favored with imidazole and triazole derivatives, whereas the most stable adduct 4' refers to imidazoline, in line with literature data.^{6c} This is a

Table 4. Relative Free Energies (kJ mol^{-1}) for the Formation of the Breslow Intermediate between *o*-Bromobenzaldehyde 2' and Carbenes 1a–d

ΔE^*	imidazole		thiazole		triazole		imidazoline	
	direct	inverse	direct	inverse	direct	inverse	direct	inverse
1+2'→3'	14.1	106.4	21.0	86.9	9.3	66.0	38.7	116.4
3'→4'	85.9	37.1	87.4	87.9	83.2	60.4	113.4	105.0

ΔE	imidazole		thiazole		triazole		imidazoline	
	direct	inverse	direct	inverse	direct	inverse	direct	inverse
4'+ ³ O ₂ →7'(t)		-214.1		-161.3		-222.1		-178.4
7'(t)→7'(s)		-78.9		-30.6		-24.6		-18.8

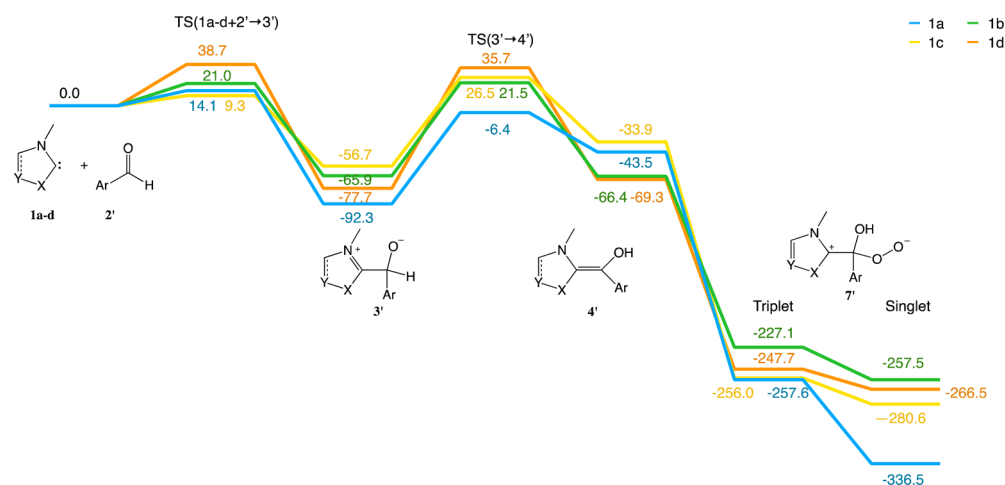


Figure 4. Energy profile for the transformations 1a–d→7' and 1a→7''. Chemical structures for intermediates are shown. The profile is to scale. It is remarkable that the path relative to the carbene 1b that is derived from a nonaromatic heterocyclic system (imidazoline) presents energy barriers very different (and higher) than the ones of the aromatic derived carbenes 1a,c,d. Energies in kJ mol^{-1} .

particularly relevant information in agreement with the observation of this key intermediate in gas phase. The overall process of the formation of 4' is exothermic.

The Breslow intermediate 4' is now ready to react with oxygen. This step introduces a possible stereoselection during the complex formation. When the bromine atom is in the *ortho* position, in fact, there are two possibilities: ³O₂ enters from the same side (*syn*) of the bromine atom or from the opposite one (*anti*), leading to two different 7'. Both cases have been considered. The two structures are conformers (through rotation of the phenyl group). The most energetically stable conformer is always the *syn* one for all the NHCs considered in this study; thus, only this conformer is reported in Table 4.

A parallel computational sequence has been performed for *p*-bromobenzaldehyde 2'', and the two sets of calculations have been compared. Figure 5 and Table 5 report the pertinent results using the imidazolium-based NHC 1a as the exemplary catalyst. The most distinctive feature in the reaction pathways characterizing the two substrates 2' and 2'' relates to the significant difference of the intermediates arising in the activation of ³O₂. In the two *ortho syn/anti* adducts, ³O₂ bonds to the C(1) atom, leading to a superoxide like structure 7', while in the case of *p*-bromobenzaldehyde the proton is removed from the OH group bonded to the same carbon atom, leading to a hydroperoxidic structure 7''. The nonexistence of the other structures has been verified computationally. *Ortho* arrangements for other NHCs, considered in this paper, present the same structure.

Therefore, it is evident that the position of the bromine atom on the aldehyde phenyl ring dramatically affects the chemical

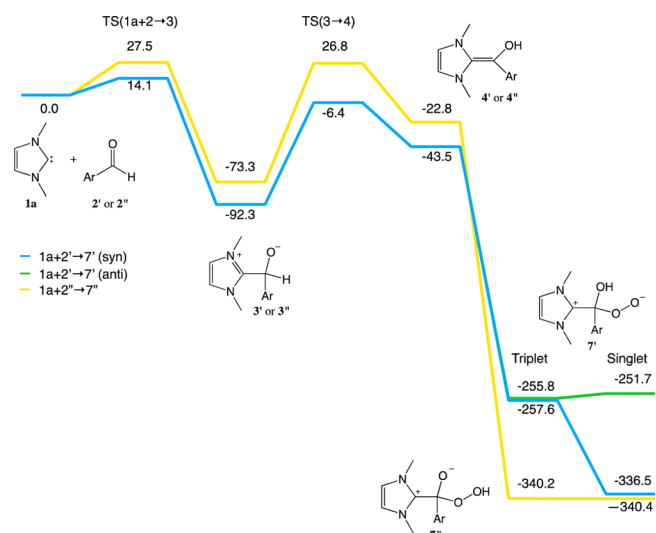


Figure 5. Energy profile for the transformations 1a→7' and 1a→7''. Chemical structures for intermediates are shown. The profile is to scale. This profile shows the different reactivity of *ortho* (2') and *para* (2'') substituted substrates. It shows also that the attack of the oxygen molecule to 4' occurs from the same side of the bromine substituent. Energies in kJ mol^{-1} .

behavior of the Breslow intermediate 4 in the oxidation process. However, to obtain further information about this phenomenon we have analyzed the electronic structure of the 4+³O₂ complexes. In our previous paper,^{14a} we reported the spin distribution for a solvent-less model. The new calculations

Table 5. Relative Free Energies (kJ mol⁻¹) for the formation of the Breslow Intermediate between *o*-Bromobenzaldehyde 2' or *p*-Bromobenzaldehyde 2'' and Carbene 1a

ΔE^*	ortho		para	
	direct	inverse	direct	inverse
1+2→3	14.1	106.4	27.5	100.8
3→4	66.9	49.9	100.1	49.6

ΔE	ortho		para
	syn	anti	
4+ ³ O ₂ →7'(t)	-214.1	-212.3	4+ ³ O ₂ →7''(t)-317.4
7'(t)→7'(s)	-78.9	4.1	7'(t)→7''(s)-0.2

confirm the transfer of an electron from the Breslow intermediate to the oxygen fragment as first stage of the oxidation process. With respect to the orbitals hosting the two unpaired electrons, the one having higher energy, is localized on the Br-C₆H₄ fragment. Calculations performed at the same level of theory on bromobenzene show that this orbital corresponds to the HOMO orbital of bromobenzene in the case of the two conformers of the *ortho* isomer and to the LUMO+1 orbital for the *para* isomer. Bromobenzene orbitals are reported in the bottom of Figure 6 for a visual comparison.

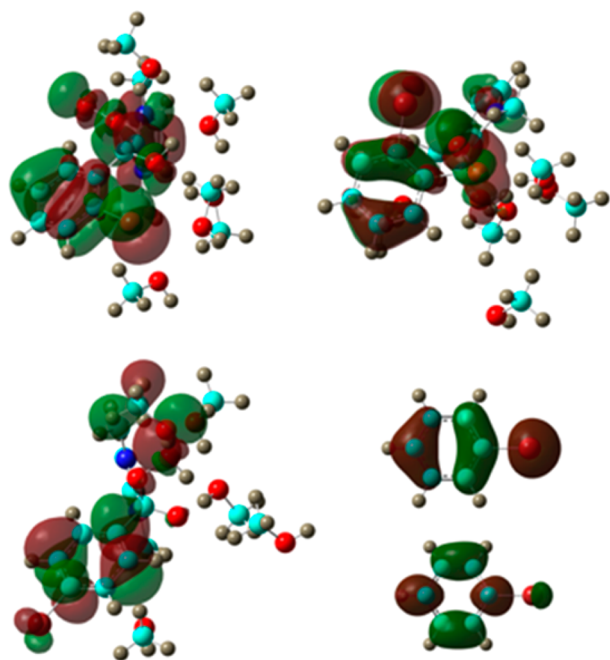


Figure 6. Geometrical structures of 4+³O₂ complexes: *anti-ortho* (top/left), *syn-ortho* (top/right), and *para* (bottom/left). Orbitals with unpaired electrons are shown (threshold value: 0.03 au). For comparison purposes, the HOMO (top) and LUMO+1 (bottom) orbitals of bromobenzene are also reported.

In particular, in the case of the *para* isomer there is a component of the orbital that is localized on the C1 atom directly bonded to the aromatic ring. The orientation of this orbital, as well as the dimension of the orbital lobe localized on the bromine atom, depends on the bromine position and therefore they are different for the two considered compounds. On the other hand, the other spin-unpaired orbital is significantly different in the *para* complex with respect to the *ortho* one: it is localized on the O-O fragment and on the nearby methanol molecule in the *para* complex and is spread

on the O-O, OH, and imidazolic fragments in the *ortho* isomer.

Consequently, it is possible to state that different positions of the bromine atom on the phenyl ring change the orientation of the molecular orbitals localized on this region, changing qualitatively the electronic structure of 7'(t)/7''(t). This feature determines the geometry and reactivity of the system. Although the presence of the same substituent in the *ortho* and *para* position is generally thought to exert a similar electronic effect, the case considered here apparently breaks this well-established concept. As expected, steric effects are significantly different in the case of *ortho* and *para* isomers. Bromine is a large and electron-rich atom that lies far from the reactive moiety of the Breslow complex in the case of the *para* isomer and close (or very close for the *syn* isomer) in the case of *o*-bromo complex. Furthermore, the orientation and the nature of the single occupied HOMO orbital is affected by the bromine atom position without any analogy between *ortho* and *para*.

Since the final products do not have a radical-like nature at some stage of the process, an intersystem crossing process, e.g., a nonradioactive transition from triplet to singlet, occurs. The candidate stage is this: the triplet state of molecular oxygen is strictly related to its symmetry. When the symmetry is broken (as in almost any reaction of ³O₂) the triplet state becomes unstable, especially in the condensed phase where third body processes (e.g., collision with solvent molecules) occur very easy. We have optimized the geometries of the two *syn/anti ortho* conformers and of the *para* isomers of 7'(s)/7''(s) starting from the corresponding triplets. There are only small differences from a geometrical point of view, but the stabilization energies are very different. The differences in energy of the two *ortho* conformers diverge significantly. While the 7'(s) *anti* conformer even is less stable than the corresponding 7'(t) complex (a situation resembling molecular oxygen) the *syn* isomer shows a stabilization energy of 78.9 kJ/mol. In the *para* case, there is only a small energetic stabilization related to the triplet quenching. The less stable *anti* conformer of *ortho* 7'(s) complex will not be considered further in this paper.

Intermediate 7 is the point of dissection of two mechanisms: the oxidative mechanism, leading to an ester, and the oxygenative mechanism leading to a carboxylic acid. *p*-Bromobenzaldehyde follows preferentially the oxidative path through the elimination of a HOO⁻ ion from 7''(s) and transformation into 10. Dissociation of a zwitterion (ion pair) requires a remarkable electrostatic work. In addition, HOO⁻ is a very strong base and nucleophile. However, in a more realistic medium (and therefore model) the presence of species able to capture this leaving anion could favor the process. Since electrophilic species of this type are not present in our model system, we decided to try to add a second aldehyde molecule that could act as a receiver. An encounter complex between 7''(s) and the added *p*-bromobenzaldehyde molecule (7''(s)+2'') has been optimized. A second encounter complex, arising from the migration of the HOO⁻ group from the oxidized Breslow complex to the aldehyde molecule (2''-OOH) was obtained. The geometric structures of the two encounter complexes and of the climbing image are shown in Figure 7.

Note that the HOO⁻ group migrates with an ancillary methanol molecule. A geometrical inspection of the structures characterizing this reaction path shows that the leaving anion has to "circumnavigate" one of the methyl groups bonded to the imidazol-2-ylidene ring to reach the other aldehyde

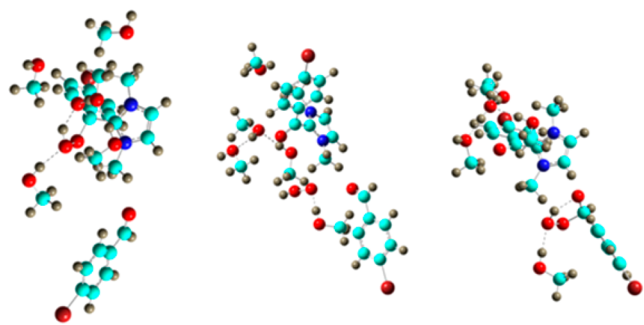


Figure 7. From left to right: geometrical structures of EC(7''(s)+2''), climbing image, and EC(10+2-OOH).

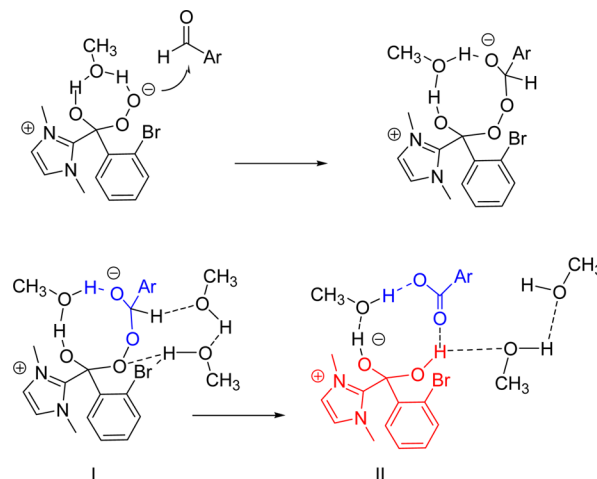
molecule and, at both extremes of the reaction path, the HOO[−] group forms a five-membered ring with the carbonyl oxygen and a hydrogen bond with a methanol molecule. From an electrostatic point of view, EC(7''(s)+2'') is constituted by two neutral molecules. The NBO analysis indicates that the complex between the hydroperoxide anion and its ancillary methanol molecule is about -0.83 , while 7''(s) carries an almost equivalent charge of opposite sign. The final complex is therefore an ion pair: the opposite charges have a magnitude of 0.88 . In **10**, almost all of the positive charge is carried out by the imidazolic fragment. EC(10+2-OOH) is less stable than EC(7''(s)+2'') at only 17.73 kJ/mol. The reaction barrier for this process is, however, considerably higher (253.69 kJ/mol), although the introduction of other explicit solvent molecules, which take into account of all the solvation effects, could significantly reduce it. The structure of 2''-OOH is analogous of the hydrate form of an aldehyde, that could be in rapid equilibrium with the formal reagents aldehyde and HOO[−]. Attempts to detect the hydrogen peroxide anion, however, have been unsuccessful.

In contrast, the *o*-bromobenzaldehyde 2' prefers the oxygenative pathway via the nucleophilic attack of the high reactive C–O–O[−] moiety to an external aldehyde molecule, followed by H-transfer, **Scheme 5**. This species **I**, stabilized by the formation of hydrogen bonds with solvent molecules, undergoes O–O bond breaking as depicted in **II** to give two new hydrogen bonded molecules, an *o*-bromobenzoic acid (in blu) and a *gem*-diol anion (in red), i.e., the oxo-Breslow **9** of **Scheme 2**; see also the mass spectrometry section of the **Supporting Information**. The removal of the first acid molecule and the further dissociation of the remaining oxo-Breslow leads to the second molecule of substituted benzoic acid and to the regeneration of the catalyst. The specific role exerted by the solvent is worthy of note.

It is not surprising, considering the reactivity of 7' and the well known instability of the –O–O– bridge, that the whole process is barrierless, except for a small energetic gap (44.19 kJ/mol) after the bridged intermediate. This is indeed the fast step of the quenching process of the C–O–O– moiety, which in the other pathway occurs simultaneously to the oxidation process. **Figure 8** displays some geometric structures.

As previously stated, the transfer of an electron from the Breslow intermediate to the molecular oxygen represents the first segment of the oxidation process. The location of the radical on the organic moiety depends on the position of the bromine substituent on the aromatic ring and corresponds to the HOMO orbital of *o*-bromobenzene and to the LUMO+1 orbital for the para isomer. In a recent paper, on the coexistence

Scheme 5. Final Steps of the Oxygenative Path^a



^aTop: The reactive C–O–O– moiety attacks a second molecule of 2'. The methanol molecule displaces its hydrogen bond to the new charged center. Bottom: In a concerted mechanism, the cleavage of the O–O bond in the structure **I** occurs synchronously to a chained transfer of three hydrogen atoms. The nearby bromine atom has a stabilizing effect. In the final structure **II**, the aldehydic group of the second molecule of 2' is now oxidized to a carboxylic one (blue). The oxo-Breslow (red) has lost an oxygen atom and it is ready to be transformed in the second acidic molecule after the regeneration of the carbene catalyst. The whole process is a solvent-mediated transfer of a single oxygen atom or, in other words, the oxidation of an aldehyde by a carbene-activated peracid.

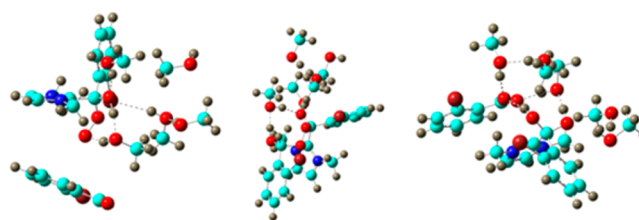
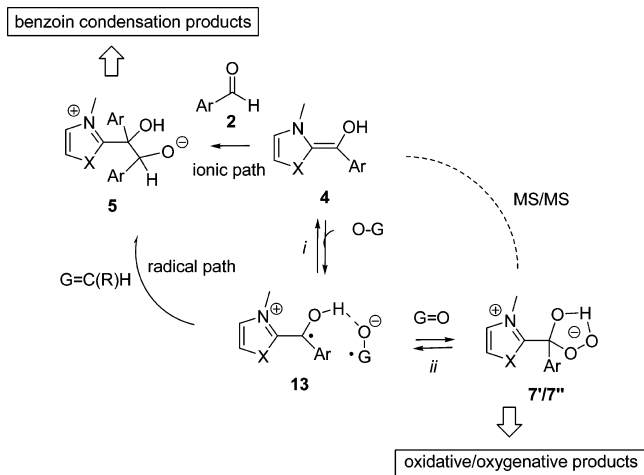


Figure 8. From left to right: Encounter complex between the *ortho* isomer of 7' and a second *o*-bromobenzaldehyde molecule 2'. –O–O– bridged intermediate (see **Scheme 5**, first row right), final complex (see **Scheme 5**, second row, right).

of ionic and radical steps in the benzoin condensation, Rehbein and co-workers^{8a} claimed that “the discovered radical intermediates can be understood as a link between other reactivities that have been exploited for instance in oxidative transformations of aldehydes via NHC-catalysis”. Our results represent an example of the mentioned oxidative transformations, and this reactivity shares important similarities with the benzoin condensation enabling the proposal for a common mechanism depicted in **Scheme 6**.

The Breslow intermediate **4** is engaged in a single-electron transfer (SET) process with an acceptor (OG = molecular oxygen or aldehyde) to afford a radical-ion pair species **13**. The radical couple, held together through hydrogen bonding, differs in structure but share the same attitude to form a new bond: O–C in the peroxidic intermediates 7'/7'' or C–C in the benzoin intermediate **5**. The likely existence of an equilibrium between the genuine Breslow intermediate **4** and both **13** and 7'/7'' (steps i and ii) is supported by electrospray mass spectrometric results that indicate the loss of O₂ [7'b→4b] during the MS/MS decomposition of 7'b that starts to be

Scheme 6. Combined N-Heterocyclic Carbene Catalysis with Aldehydes under Anaerobic (Benzoin) and Aerobic (Oxidative/Oxygenative) Conditions



detected for relatively low excitation voltages of ca. 20 mV, Figure 9. An analogous equilibrium of **4** with **13**, in the case $G = C(R)H$, has been proposed as prerequisite for the concurrence of ionic and radical steps in the classical benzoin condensation.^{8a}

CONCLUSIONS

The reaction paths and the intermediate structures related to the formation of the Breslow intermediate and its oxidation along the oxidative/oxygenative paths have been studied from a mechanistic point of view, with the support of gas phase and computational studies. The position of the bromine substituent on the aromatic ring of aldehyde substrate leads to small energetic and structural differences on the two-step process related to the formation of the Breslow intermediate, intercepted and characterized as the enol structure by ESI-MS/MS experiments. Our calculations confirm the transfer of an electron from the Breslow intermediate **4** to the oxygen fragment as first stage of the oxidation process. From the recombination of $[4]^{*+}$ and $[O_2]^{*-}$, that arise from the SET process, two distinct peroxidic tautomeric structures are formed, as a consequence of the position of the substituent

on the aromatic ring. These structures have a divergent reactivity. The proton displacement, occurring in the *p*-bromobenzaldehyde, makes it impossible for this isomer to follow the oxygenative path. On the other hand, we cannot exclude that, for the *ortho* isomer, this process takes place concurrently to the bimolecular reaction here reported. The specific role of the solvent (methanol) has been demonstrated. Overall, computational and gas phase results are fully consistent with the reactivity observed in solution. The proposed mechanism shares important similarities with that one of the recently revisited benzoin condensation.

EXPERIMENTAL SECTION

Liquid aldehydes were freshly distilled before their utilization. Reactions were monitored by TLC on silica gel 60 F254 with detection by charring with phosphomolybdic acid. Flash column chromatography was performed on silica gel 60 (230–400 mesh). 1H (400 MHz) and ^{13}C (100 MHz) NMR spectra were recorded in D_2O or $DMSO-d_6$ solutions at room temperature. Peaks assignments were aided by 1H – 1H COSY and gradient-HMQC/HMBC experiments.

1,1'-(Hexane-1,6-diyl)bis(3-methyl-1*H*-imidazolium) Bromide **11a(Br₂).** 1-Methylimidazole (1.50 g, 18.3 mmol) and 1,6-dibromohexane (1.78 g, 7.30 mmol) were first mixed at room temperature for 20 min and then heated at 100 °C for 2 h. The resulting mixture was cooled to room temperature, triturated with Et_2O , and filtered. The resulting white solid was stirred for 1 h in $EtOAc$ (15 mL), filtered, and dried in vacuo. The desired salt **11a-Br** (77%, 2.30 g) was obtained as an amorphous solid. 1H NMR (400 MHz, D_2O): δ = 8.60 (s, 2 H, 2 NCHN), 7.35 (m, 4 H, 2 NCHCHN), 4.04 (t, 4H, J = 7.2 Hz, 2 NCH₂), 3.74 (s, 6 H, 2 NCH₃), 1.72 (m, 4 H, 2 NCH₂CH₂), 1.19 (br s, 4 H, 2 NCH₂CH₂CH₂). $^{13}C\{^1H\}$ NMR (100 MHz, D_2O): δ = 135.7 (NCHN), 123.4 (CH₂N), 122.1 (CH₂N), 49.3 (CH₂N), 35.6 (CH₃N), 29.0 (CH₂), 24.7 (CH₂). HRMS for $[11a(Br)]^+$ C₁₄H₂₄N₄Br: found 327.1180, calcd 327.1179.

1,1'-(Hexane-1,6-diyl)bis(3-methyl-4,5-dihydro-1*H*-imidazolium) Bromide **11b(Br₂).** 1-Methyl-4,5-dihydro-1*H*-imidazole²⁶ (1.50 g, 17.8 mmol) and 1,6-dibromohexane (1.90 g, 7.80 mmol) were first mixed at room temperature for 20 min and then heated at 100 °C for 3 h. The resulting mixture was cooled to room temperature, dissolved in $EtOH$ (15 mL), precipitated by the addition of Et_2O , decanted, and dried in vacuo. The desired salt **11b-Br** (68%, 2.20 g) was obtained as a sticky solid. 1H NMR (400 MHz, D_2O): δ = 8.34 (s, 2 H, 2 NCHN), 3.97 (br s, 8 H, 2 NCH₂CH₂N), 3.50 (t, 4 H, J = 7.1 Hz, 2 NCH₂), 3.19 (s, 6 H, 2 NCH₃), 1.72 (m, 4 H, 2 NCH₂CH₂), 1.42 (m, 4 H, 2 NCH₂CH₂CH₂). $^{13}C\{^1H\}$ NMR (100 MHz, D_2O): δ = 159.1 (NCHN), 51.6 (CH₂N), 49.7 (CH₂N), 48.9

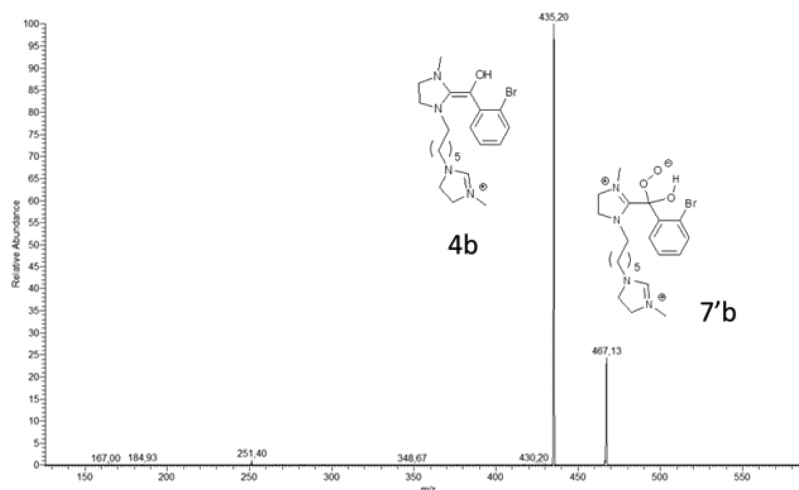


Figure 9. MS/MS spectrum of the peroxo Breslow **7'b** at m/z 467 (^{79}Br).

(CH₂N), 35.1 (CH₃N), 27.9 (CH₂), 26.7 (CH₂). HRMS for [11b(Br)]⁺ C₁₄H₂₈N₄Br: found 331.1492, calcd 331.1492.

4,4'-(Hexane-1,6-diyl)bis(1-methyl-1,2,4-triazolium) Bromide 11c(Br₂). To solution of 1-methyl-1,2,4-triazole (810 mg, 0.01 mol) in acetonitrile (5 mL), cooled in an ice bath, was added 1,6-dibromohexane (1.2 g, 0.05 mol). After the addition was complete, the ice bath was removed, and the reaction mixture was stirred at reflux temperature for 24 h and then concentrated. The resultant white solid, 3,3'-dimethyl-1,1'-(hexane-1,6-diyl)-1,2,4-ditriazolium bromide **11c-Br**, was washed with ether (3 × 50 mL) and dried under vacuum for 1 h. ¹H NMR (D₂O): δ = 9.77 (s, 2 H), 8.85 (s, 2 H), 4.32 (q, J = 7.3 Hz, 4 H), 4.12 (s, 6 H), 1.93 (m, 4 H), 1.41 (m, 4 H). ¹³C{¹H} NMR (100 MHz, D₂O): δ = 144.4, 142.1, 47.9, 38.5, 28.5, 24.5. HRMS for [11c(Br)]⁺ C₁₂H₂₂N₄Br: found 329.1087, calcd 329.1084.

3,3'-(Hexane-1,6-diyl)bis(4-methylthiazolium) Bromide 11d(Br₂). 4-Methylthiazole (1.80 g, 18.3 mmol) and 1,6-dibromohexane (1.78 g, 7.30 mmol) were first mixed at room temperature and then heated at 100 °C for 4 h. The resulting mixture was cooled to room temperature, triturated with Et₂O, and filtered. The resulting white solid was stirred for 1 h in EtOAc (15 mL), filtered, and dried in vacuo. The desired salt **11d-Br** was obtained (74%, 2.40 g) as an amorphous solid. ¹H NMR (400 MHz, D₂O): δ = 9.68 (d, 2 H, J = 2.1 Hz, 2 NCHS), 7.66 (br s, 2 H, 2 SCH), 4.30 (t, 4 H, J = 7.6 Hz, 2 NCH₂), 2.43 (s, 6 H, 2 CH₃), 1.82 (m, 4 H, 2 NCH₂CH₂), 1.30 (m, 4 H, 2 NCH₂CH₂CH₂), ¹³C{¹H} NMR (100 MHz, D₂O): δ = 156.9 (NCHS), 146.6 (CN), 120.8 (CHS), 52.8 (CH₂N), 28.5 (CH₂), 24.9 (CH₂), 12.4 (CH₃). HRMS for [11d(Br)]⁺ C₁₄H₂₂N₂S₂Br: found 361.0404, calcd 361.0402.

General Procedure for Counterion Exchange in Azolium Salts 11a–d(Br₂). The selected dibromide salt **11a–d(Br₂)** (1.22 mmol) was dissolved in a minimal amount of water, and saturated aqueous solution of potassium hexafluorophosphate or lithium bis(trifluoromethanesulfonyl)imide (2.50 mmol) was added. The reaction mixture was stirred at room temperature for 1 day. The aqueous layer was decanted, and the remaining layer was dissolved in dichloromethane and washed with water (6 × 100 mL) until the AgNO₃ test on the aqueous phase was completely negative. The organic solvent was removed in vacuo, and the resultant liquid was dried under high vacuum. In all cases, ESI-MS spectra confirmed that Br[−], arising from incomplete reactions, were not detectable in the samples arising by exchange reactions.

General Procedure for the Aerobic Oxidation of Aldehyde 2'/'2" Catalyzed by 11a–d(X₂). A mixture of aldehyde 2' or 2" (0.40 mmol), 1,8-diazabicyclo[5.4.0]undec-7-ene (66 μL, 0.44 mmol), azolium salt **11a–d(X₂)** (0.40 mmol), activated 4-Å powdered molecular sieves (100 mg), anhydrous THF (2 mL), and anhydrous MeOH (1 mL) was warmed at 55 °C and stirred at that temperature for 16 h under air (air-filled balloon). The mixture was filtered through a pad of Celite, diluted with CH₂Cl₂ (15 mL) and 1 M HCl (5 mL), cooled to room temperature, and then poured into a separatory funnel. The organic phase was separated, and the aqueous phase was extracted with CH₂Cl₂ (3 × 15 mL). The combined organic phases were dried (Na₂SO₄) and concentrated to give the corresponding acid and/or the ester (Tables 1 and 2). The reaction conversion and acid/ester ratio was determined by ¹H NMR analysis (DMSO-*d*₆) using bromoform as the internal standard (5 mg/mL in methanol, analytical standard). The above crude mixture was eluted from a column of silica gel with 15:1 cyclohexane–AcOEt to isolate the ester and then with 10:1 AcOEt–AcOH to recover the acid.

Mass Spectrometric Experiments. (+)-ESI and MS/MS mass spectra were acquired using an ion-trap mass spectrometer equipped with an electrospray ionization source. Instrumental parameters: capillary voltage −10 V, spray voltage 4.50 kV, capillary temperature of 150 °C, mass scan range from *m/z* 50 to 1000; N₂ was used as sheath gas. The samples were injected into the spectrometer by syringe pump at a constant flow rate of 8 μL/min using THF–MeOH (2:1) as the eluting solvent. The appropriate aldehydes **2** and **1** were mixed in equimolar amounts of 10^{−3} M in the presence of DBU (1 equiv) as base. MS/MS experiments were carried out by using tickling voltages in the range 10–40 mV. The change of the eluting mixture to ACN–

MeOH (3:1) afforded very similar results. The MS data were acquired following the reaction from the early moments up to 30 min. Additional checks were carried out after 2 h.

HRMS were obtained on a Q/TOF-MS, using a quadrupole, a hexapole, and a time-of-flight unit equipped with an electrospray ionization source.

Theoretical Calculations. Calculations have been performed using version 1.5K of Terachem. The level of theory is B3LYP/6-311+G(d,p) with D2 dispersion correction. The calculations were performed on a workstation equipped with four NVIDIA GeForce GTX Titanium GPUs.

■ ASSOCIATED CONTENT

📄 Supporting Information

The Supporting Information is available free of charge on the ACS Publications website at DOI: 10.1021/acs.joc.6b02414.

NMR spectra, mass spectrometric experiments, DFT calculations, and absolute energies (PDF)

■ AUTHOR INFORMATION

Corresponding Authors

*E-mail: olga.bortolini@unife.it.

*E-mail: christian.pomelli@gmail.com.

ORCID

Olga Bortolini: 0000-0002-8428-2310

Cinzia Chiappe: 0000-0001-6615-908X

Notes

The authors declare no competing financial interest.

■ ACKNOWLEDGMENTS

We gratefully acknowledge the University of Ferrara (Fondi FAR) for financial support. Thanks are also given to Mr. P. Formaglio for NMR spectroscopic experiments and to Dr. T. Bernardi for high-resolution mass spectrometric experiments.

■ REFERENCES

- (1) (a) Flanigan, D. M.; Romanov-Michailidis, F.; White, N. A.; Rovis, T. *Chem. Rev.* **2015**, *115*, 9307–9387. (b) Hopkinson, M. N.; Richter, C.; Schedler, M.; Glorius, F. *Nature* **2014**, *510*, 485–496. (c) Bugaut, X.; Glorius, F. *Chem. Soc. Rev.* **2012**, *41*, 3511–3522. (d) Moore, J. L.; Rovis, T. *Top. Curr. Chem.* **2009**, *291*, 77–144. (e) Enders, D.; Niemeier, O.; Henseler, A. *Chem. Rev.* **2007**, *107*, 5606–5655.
- (2) Breslow, R. *J. Am. Chem. Soc.* **1958**, *80*, 3719–3726.
- (3) Lapworth, A. *J. Chem. Soc., Trans.* **1903**, *83*, 995–1005.
- (4) (a) Goldfuss, B.; Schumacher, M. *J. Mol. Model.* **2006**, *12*, 591–595. (b) Schumacher, M.; Goldfuss, B. *Tetrahedron* **2008**, *64*, 1648–1653.
- (5) (a) Hawkes, K. J.; Yates, B. F. *Eur. J. Org. Chem.* **2008**, *2008*, 5563–5570. (b) He, Y.; Xue, Y. *J. Phys. Chem. A* **2011**, *115*, 1408–1417.
- (6) For a solvent-mediated proton transfer, see: (a) He, Y.; Xue, Y. *J. Phys. Chem. A* **2010**, *114*, 9222–9230. (b) Ajitha, J.; Suresh, C. H. *Tetrahedron Lett.* **2013**, *54*, 7144–7146. (c) Schumacher, M.; Goldfuss, B. *New J. Chem.* **2015**, *39*, 4508–4518. (d) Zhang, W.; Wang, Y.; Wei, D.; Tang, M.; Zhu, X. *Org. Biomol. Chem.* **2016**, *14*, 6577–6590.
- (7) For a possible involvement of a spiroepoxide intermediate, see: (a) Gronert, S. *Org. Lett.* **2007**, *9*, 3065–3068. (b) Berkessel, A.; Elfert, S. *Adv. Synth. Catal.* **2014**, *356*, 571–578. (c) Buzsáki, D.; Kelemen, Z.; Nyulászi, L. *Struct. Chem.* **2016**, *27*, 1569–1576.
- (8) For radical pathways, see: (a) Rehbein, J.; Ruser, S.-M.; Phan, J. *Chem. Sci.* **2015**, *6*, 6013–6018. (b) Alwarsh, S.; Xu, Y.; Qian, S. Y.; McIntosh, M. C. *Angew. Chem., Int. Ed.* **2016**, *55*, 355–358.

(9) (a) Berkessel, A.; Elfert, S.; Yatham, V. R.; Neudörfel, J.-M.; Schlörer, N. E.; Teles, J. H. *Angew. Chem., Int. Ed.* **2012**, *51*, 12370–12374. (b) Berkessel, A.; Elfert, S.; Etzenbach-Effers, K.; Teles, H. *Angew. Chem., Int. Ed.* **2010**, *49*, 7120–7124.

(10) DiRocco, D. A.; Oberg, K. M.; Rovis, T. *J. Am. Chem. Soc.* **2012**, *134*, 6143–6145.

(11) (a) Maji, B.; Mayr, H. *Angew. Chem., Int. Ed.* **2012**, *51*, 10408–10412. (b) Maji, B.; Horn, M.; Mayr, H. *Angew. Chem., Int. Ed.* **2012**, *51*, 6231–6235.

(12) Tian, Y.; Lee, J. K. *J. Org. Chem.* **2015**, *80*, 6831–6838.

(13) For reviews on NHC catalysis under oxidative conditions, see (a) De Sarkar, S.; Biswas, A.; Samanta, R. C.; Studer, A. *Chem. - Eur. J.* **2013**, *19*, 4664–4678. (b) Knappke, C. E. I.; Imami, A.; von Wangelin, A. *J. ChemCatChem* **2012**, *4*, 937–941. See also: (c) Vora, H. U.; Wheeler, P.; Rovis, T. *Adv. Synth. Catal.* **2012**, *354*, 1617–1639. (d) Green, R. A.; Pletcher, D.; Leach, S. G.; Brown, R. C. D. *Org. Lett.* **2016**, *18*, 1198–1201. (e) Samanta, R. C.; Studer, A. *Org. Chem. Front.* **2014**, *1*, 936–939.

(14) (a) Bortolini, O.; Chiappe, C.; Fogagnolo, M.; Giovannini, P. P.; Massi, A.; Pomelli, C. S.; Ragno, D. *Chem. Commun.* **2014**, *50*, 2008–2011. (b) Zhao, J.; Mück-Lichtenfeld, C.; Studer, A. *Adv. Synth. Catal.* **2013**, *355*, 1098–1106. (c) Möhlmann, L.; Ludwig, S.; Blechert, S. *Beilstein J. Org. Chem.* **2013**, *9*, 602–607. (d) Reddi, R. N.; Malekar, P. V.; Sudalai, A. *Tetrahedron Lett.* **2013**, *54*, 2679–2681. (e) Kiran, I. N. C.; Lalwani, K.; Sudalai, A. *RSC Adv.* **2013**, *3*, 1695–1698.

(15) Zeng, H.; Wang, K.; Tian, Y.; Niu, Y.; Greene, L.; Hu, Z.; Lee, J. K. *Int. J. Mass Spectrom.* **2014**, *369*, 92–97.

(16) Schrader, W.; Handayani, P. P.; Burstein, C.; Glorius, F. *Chem. Commun.* **2007**, 716–718.

(17) Studer, A.; Curran, D. P. *Angew. Chem., Int. Ed.* **2016**, *55*, 58–102.

(18) Corilo, Y. E.; Nachtigall, F. M.; Abdelnur, P. V.; Ebeling, G.; Dupont, J.; Eberlin, M. N. *RSC Adv.* **2011**, *1*, 73–78.

(19) Collett, C. J.; Massey, R. S.; Taylor, J. E.; Maguire, O. R.; O'Donoghue, A. M. C.; Smith, A. D. *Angew. Chem., Int. Ed.* **2015**, *54*, 6887–6892.

(20) For other examples of SET mediated reactivity on NHC, see: (a) Guin, J.; De Sarkar, S.; Grimme, S.; Studer, A. *Angew. Chem., Int. Ed.* **2008**, *47*, 8727–8730. (b) White, N. A.; Rovis, T. *J. Am. Chem. Soc.* **2014**, *136*, 14674–14677. (c) Du, Y.; Wang, Y.; Li, X.; Shao, Y.; Li, G.; Webster, R. D.; Chi, Y. R. *Org. Lett.* **2014**, *16*, 5678–5681. (d) Zhang, Y.; Du, Y.; Huang, Z.; Xu, J.; Wu, X.; Wang, Y.; Wang, M.; Yang, S.; Webster, R. D.; Chi, Y. R. *J. Am. Chem. Soc.* **2015**, *137*, 2416–2419. (e) Barletta, G.; Chung, A. C.; Rios, C. B.; Jordan, F.; Schlegel, M. J. *Am. Chem. Soc.* **1990**, *112*, 8144–8149. (f) Maji, B.; Mayr, H. *Angew. Chem., Int. Ed.* **2012**, *51*, 10408–10412. (g) Nair, V.; Bindu, S.; Sreekumar, V.; Rath, N. P. *Org. Lett.* **2003**, *5*, 665–667.

(21) Paul, M.; Breugst, M.; Neudörfel, J.-M.; Sunoj, R. B.; Berkessel, A. *J. Am. Chem. Soc.* **2016**, *138*, 5044–5051.

(22) Chiappe, C.; Pomelli, C. S. *Phys. Chem. Chem. Phys.* **2013**, *15*, 412–423.

(23) (a) Terachem v1.5, Petachem LLC, 2009, 2015. (b) Ufimtsev, I. S.; Martinez, T. J. *J. Chem. Theory Comput.* **2009**, *5*, 2619–2628.

(24) Goerigk, L.; Grimme, S. *Phys. Chem. Chem. Phys.* **2011**, *13*, 6670–6688.

(25) Kästner, J.; Carr, J. M.; Keal, T. W.; Thiel, W.; Wander, A.; Sherwood, P. J. *Phys. Chem. A* **2009**, *113*, 11856–11860.

(26) Bessel, M.; Rominger, F.; Straub, B. F. *Synthesis* **2010**, 1459–1466.